



Accuration of Measurement Snake Motion Based on Kalman Filter Sensor Fusion

Fathurozi Winjaya¹ Dara Aulia Feryando² Nur Annisa Azizah³
^{1,2,3}Politeknik Perkeretaapian Indonesia Madiun, Madiun, Indonesia
fathurrozi@ppi.ac.id

Abstract Snake motion is a movement on a pair of rail wheels that does not go straight forward but shifts to the left or right. Snake movement can cause deformation on the rail and weariness on the wheel. The snake motion can be measured using sensors that have a high sensitivity but are at risk for noise in the data readings. The control system will not be able to perform at its best when the volume measurements are counted as input data from the measurement. From the application of the filter algorithm to the combination of the sensor accelerometer and gyroscope obtained results, noise measurement can be minimised and data reading more stable. The result of noise reduction depends on the value of the process variance; if the process variant value is close to 0, then the filtering result carried out by the filter valve is more smooth. The filter column with the 0.025 process variant produces an average error value of 3.9% on the x axis, 3.1% on the y axis, and 5.7% on the z axis. With the highest error on the measurement at the 30° parameter with the measuring difference of 1.27° at the x-axis, the 60° parameters with the measured gap of 1.34° in the y-axis, and the -90° parametrics with a measuring gap of 2.99° on the Z-axial.

Keywords : Snake motion, Accelerometer, Gyroscope, Sensor fusion, Kalman Filter.

1. Introduction

Snake motion is due to the movement of a pair of wheels that are not moving straight forward but shifting on the left or right side [1]. Snake movement has an impact on the winding of the wheel. Because of the snake movement that forces the wheel to move to the left and right, the winds of the flange wheel and the rail on the straight path will be divided evenly between the right and the left [2]. So the measurement of snake motion can be done to help in the implementation of maintenance of railway equipment and facilities on a regular basis.

A sensor is a device to detect or measure the magnitude of mechanical, magnetic, heat, radiation, and chemical variations converted into electrical voltage and current [3]. Sensors with high sensitivity are so susceptible to environmental noise when reading data because sensors usually do not have protection from external interference such as wind pressure and vibration. Well, noise from sensor readings should be suppressed or eliminated as much as possible. However, it is hardly possible to eliminate noise altogether because it occurs due to the nature of the environment from the outside. Another option is to reduce noise or to separate noise from actual measurement data. Noise on data readings can have serious consequences, leading to the control system not achieving its best

performance or also causing the system to fail to be controlled if noise is counted as measurement data. According to Kalman filters are capable of performing noise reduction very well [4]. Thus, in this study, the Kalman filter was selected and used as a support to reduce noise in the sensing process carried out by a fusion sensor that has high sensitivity to measure snake motion.

2. Research Methods

2.1 Sensor Fusion

A sensor fusion is a method of merging data obtained from the results of a single sensor reading into a single unit of information in a comprehensive way so that the given result can be better and more accurate when compared to autonomous sensor measurement [5].

2.2 Kalman Filter

The Kalman filter is an autoregressive filtering model because estimates of current time conditions can be obtained from estimates from previous systems and observations of the current time system. [6]. Kalman Filter has two parts: prediction and correction.

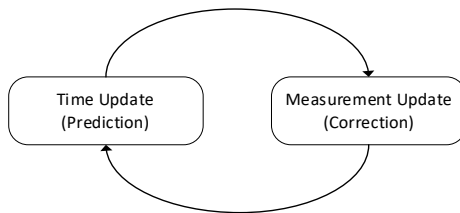


Fig. 1. Cycle of Kalman Filter

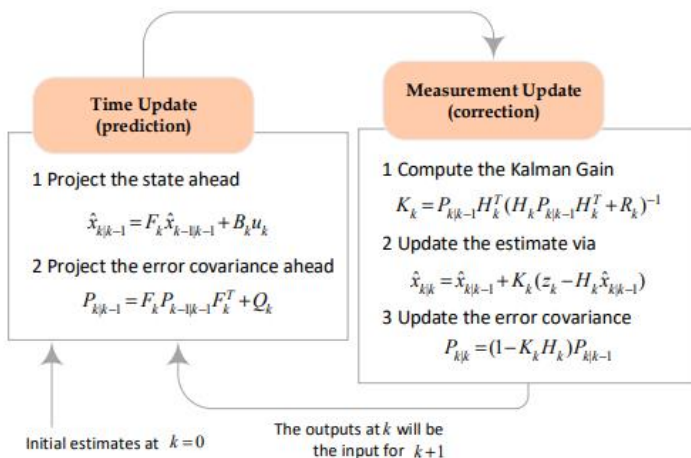


Fig. 2. Process of Kalman Filter

The formula Kalman Filter equation is shown at (1) – (5):

Update

$$\hat{X}_{t|t-1} = F_t \hat{X}_{t-1|t-1} + B_t u_t$$

(1)

$$P_{t|t-1} = F_t P_{t-1|t-1} F_t^T + Q_t$$

(2)

Correction

$$\hat{X}_{t|t} = \hat{X}_{t|t-1} + K_t (y_t - H_t \hat{X}_{t|t-1})$$

(3)

$$K_t = P_{t|t-1} H_t^T (H_t P_{t|t-1} H_t^T + R_t)^{-1}$$

(4)

$$P_{t|t} = (1 - K_t H_t) P_{t|t-1}$$

(5)

The estimate system in the Kalman Filter is divided into two parts: update and predict. The predict part works with the system using the results of the prediction of the system state in the previous time to predict the current state. The basic equation of the target filter is not defined, so it needs to be modified for more specific purposes [7].

2.3 Snake Motion

The snake movement on the railway is due to the movement of the wheel pair, which does not go straight forward but shifts to the left or right [1]. Irregular wheel movements moving left and right will cause deformation on the track. The lateral style caused by the wheel cannot be held by the track and consequently will be deformed [8].

3. Methods

3.1 Hardware Design

In the hardware design, this contains information about the design description of each series of hardware that will lead to the manufacture of the tool. On the block diagram of the system, the way the tool works is a diagram that describes the part of the workflow of a system that is made. The workflow starts from input to output according to the

specifications of the planned tool operating system.



Fig. 3. System block diagram

Figure 3 describes a system block diagram of how the tool works. The final task of this research was to design a prototype of the combination of the accelerometer sensor and the gyroscope by applying the Kalman Filter algorithm. The data obtained from the input of the accelerometer and gyroscope sensors in the MPU 6050 module will be transmitted via I2C communication to the ADC on the Arduino Uno microcontroller to be converted into digital data. The digital data read by the Arduino Uno microcontrollers will then be used by the IDE application to run the Kalman Filter algorithm. This will allow the accelerometer and gyroscope to work together to provide measurement data. Process how the system works is shown in Figure 4

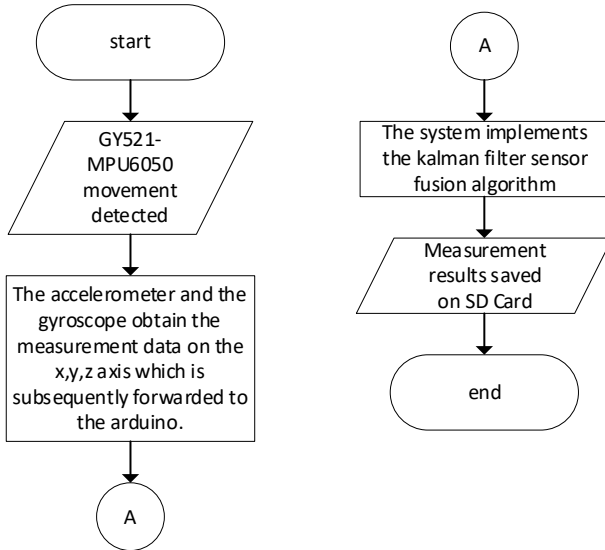


Fig. 4. Flowchart the system

3.2 Software Design

The accelerometer sensor is a good sensor used to monitor motion. It is able to give accurate values in static conditions but has a slow response when following fast movements [9]. So this study combined accelerometer measurement data with a gyroscope to get better measurements. The following is a diagram of the concept of combining sensor data with the Kalman Filter algorithm. From the diagram in Figure 5, it is clear that this

sensor combination is done by combining the data from the accelerometer and gyroscope measurement results using the Kalman filter algorithm. The final result of this study is that the sensor can measure an object with minimal noise after applying a Kalman Filter.

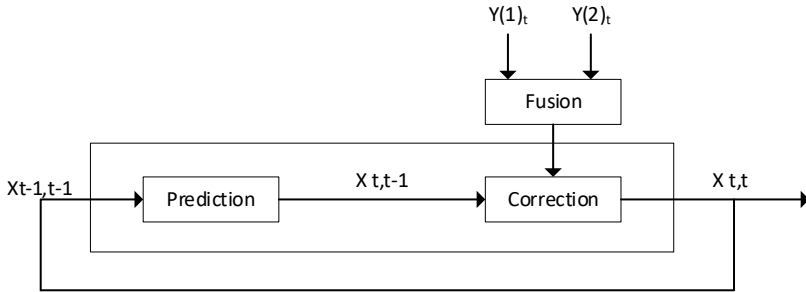


Fig. 5. Sensor Combination Diagram With Kalman Filter

The Kalman Filter data processing process diagram in Figure 5 is used to explain the workflow of Kalman Filter on the measurement of the combined sensor accelerometer and gyroscope. The first phase of the Kalman Filter performed is initial initialization, where at this stage it is performed only once in each measurement. This phase also uses two parameters, namely system initial status $X_{0|0}$ and initial state uncertainty $P_{0|0}$, and at this stage is followed by prediction. Then go to the first measurement phase, where you have to provide two parameters, namely the P_t uncertainty measurement update process and also the input data from the sensor readings that will be input data on the y_t system. The input entered at this stage is the value of the y_t sensor readings, the R_t measurement uncertainty, the state estimate of previous measurements $X_{t|t-1}$ and the uncertainty estimate $PP_{t|t-1}$. Based on the input, the status update process will calculate the word gain, which subsequently yields two outputs, namely the current state estimates $X_{t|t}$ and the current circumstances estimates $P_{t|t}$ calculated using the estimate update equation. This parameter is the output that always exists on the filter slate. Next is the prediction stage; this is the final stage of the estimation using the filter Slate. Where the uncertainty of the state estimate begins to be calculated for the next system based on the dynamic model of the system $X_{t+1|t} = X_{t|t}$ and extrapolates the current system state $P_{t+1|t} = P_{t|t}$. In the first repetition, the output from the initialization is treated as the estimate and uncertainty of the previous state. In the next iteration, the prediction output treats the estimates and uncertainties of the preceding state.

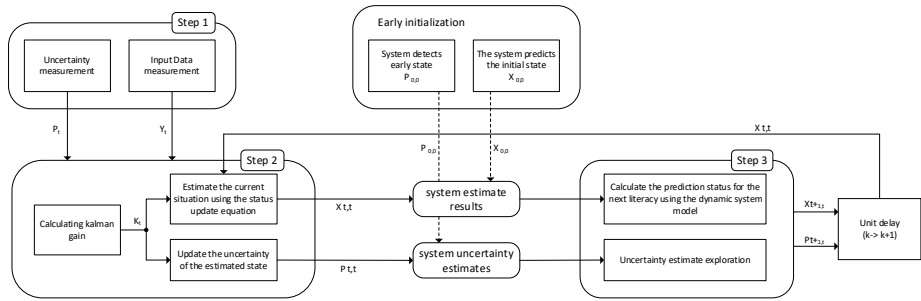


Fig. 6. Data Processing Diagram Kalman Filter

4. Result

4.1 Sensor Calibration

Sensor calibration functions are used to obtain sensor readings with high accuracy and precision. The instruments to be used for calibration are those that have already obtained a proper licence for sale for public procurement or that have been certified nationally or internationally. The test aims to determine the measurement differential and percentage error of the measuring results of the combined sensor accelerometer and gyroscope, which has applied the algorithm of the filter with the comparator of manual measurements of the arc gradient.

Table 1. Calibration Testing

No.	Standard angle (°)	Angle measurement (°)	Measurement differential (°)	Error (%)
1.	10°	10.99	0.99	9.9
2.	-10°	-10.96	0.96	9.6
3.	30°	31.27	1.27	4.3
4.	-30°	-30.85	0.85	2.8
5.	45°	45.95	0.95	2.1
6.	-45°	-46.56	1.56	3.4
7.	60°	60.92	0.92	1.5
8.	-60°	-60.55	0.55	0.9
9.	90°	90.3	0.3	0.3
10.	-90°	93.82	3.82	4.2
error (%)				3.9

This test is done by comparing the measurement of the sensor with the measuring instrument of the degree arc gradient. Average angles are obtained from an average of 5×

measurements, where in one measurement there are more than 500 measures with a time of 5 seconds. Here is a table of measurement test results for the combined accelerometer and gyroscope sensor, which has applied the Kalman Filter algorithm to the x axis.

The calculation of the percentage error of angle measurement using the combination sensor accelerometer and gyroscope can be measured with the following equation [10]:

$$\% \text{ error} = \frac{\text{value sensor} - \text{standar value}}{\text{standar value}} \times 100\% \tag{6}$$

Table 2. Data Table of Measurement on Y Axis

No.	Standard angle (°)	Angle measurement(°)	Measurement differential(°)	Error (%)
1.	10°	11.01	1.01	10.1
2.	-10°	-10.87	0.87	8.7
3.	30°	30.46	0.46	1.5
4.	-30°	-30.9	0.9	3
5.	45°	45.55	0.55	1.2
6.	-45°	-45.62	0.62	1.3
7.	60°	61.34	1.34	2.2
8.	-60°	-61.02	1.02	1.7
9.	90°	90.74	0.74	0.82
10.	-90°	-90.62	0.62	0.62
error (%)				3.1

Table 3. Data Table of Measurement on Z Axis

No.	Standard angle (°)	Angle measurement (°)	Measurement differential (°)	Error (%)
1.	10°	11.40	1.40	14
2.	-10°	-11.48	1.48	14.8
3.	30°	31.09	1.09	3.6
4.	-30°	-31.78	1.78	5.9
5.	45°	46.24	1.24	2.7
6.	-45°	-47.13	2.13	4.7
7.	60°	61.38	1.38	2.3
8.	-60°	-61.82	1.82	3.03
9.	90°	92.98	2.98	3.3
10.	-90°	-92.99	2.99	3.3
error (%)				5.7

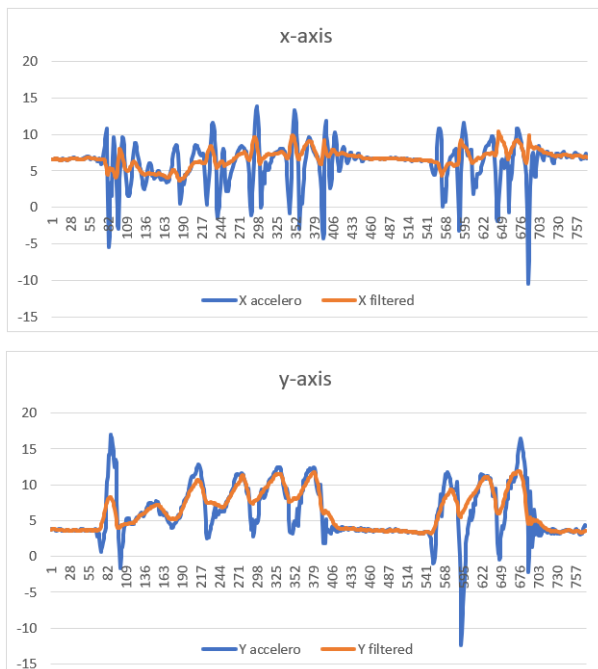
Based on the results of the x, y, and z axis accuracy tests shown in tables 1, 2, and 3

on the x axis differential with an average reference angle of 3.9%, the minimum error was found in the 90° test with a 0.3° difference, and the maximum error was in the 30° test with a 1.27° difference. On the y axis, the difference was 3.1%; the minimal error was observed in the test at -90° with the 0.62° difference; and the maximal error was present in the 60° test at the 1.34° gap.

4.2 Kalman Filter Testing

The purpose of this test is to compare the graphics of the sensor readings that have been applied to a change in the state of the filter with the sensor reading before the filter readings are implemented. This test is done by creating a vibration around the sensor.

Figure 7 show the measurement by the sensor before applying the filter colour, and the orange colour is the measurement of the sensor already in the filter. From measurements on the three axes, it shows that the data generated by the already-implemented sensor algorithm has a more stable sensor reading. As seen from the x-axis measuring in Fig. 7, where the measures on the blue colour chart touch at figures 15 to -15 after applying the filter, the noise measuring results touch at numbers 10.



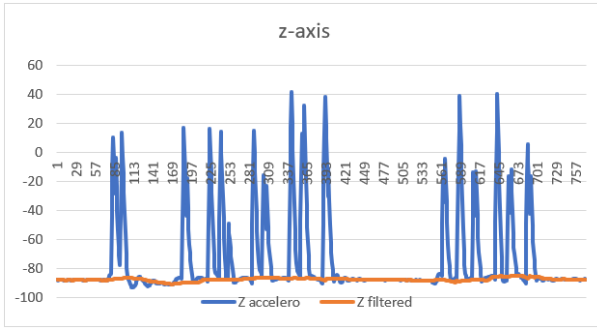
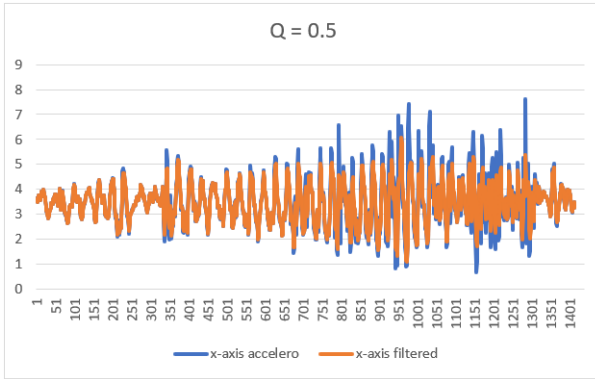


Fig. 7. Data measurement of Kalman filter

4.3 Kalman Filter Matrix Varian Testing

This test aims to see the influence of the variance value of the matrix on the measurement of the filter valve. This test is done by giving an input value of $Q = 0.5$ and giving a vibration to the sensor for 5 seconds. Based on Figure 8, the measured results are filtered on the axes x, y, and z only slightly. The measurement still has a lot of noise. Here are the test results of the Kalman Filter method with a value of $Q = 0.5$.



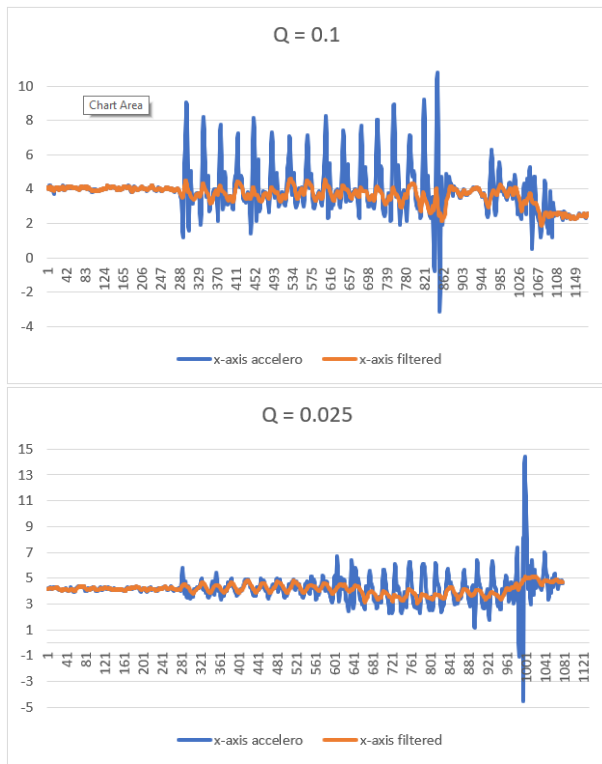


Fig. 8. Kalman Filter matrix varian testing

Based on the results of tests on axes x, y, and z, giving Q values of 0.5, 0.1, and 0.025 leads to the conclusion that the smaller the value of Q the measurement is filtered by the filter cylinder, the more stable it is. Because Q plays a role in describing the uncertainty in the change in the system state between $k-1$ and k . The larger the value in the Q matrix, the greater the unexpectedness of the changes in the state. If Q is a diagonal matrix, the elements represent uncertainties in the changing state in the corresponding dimensions. The selection of the Q matrix is an important part of the Kalman filter configuration, so it is necessary to estimate the level of uncertainty in changes in the system condition or obtain values from experiments. The Q matrix can describe system changes such as acceleration, change in speed, or other fluctuations in changing circumstances.

4.4 Snake Motion Testing

The purpose of the test is to find out the results of the sensor measurement against snake motion. The test was carried out using a push truck with a delay of 100 ms.

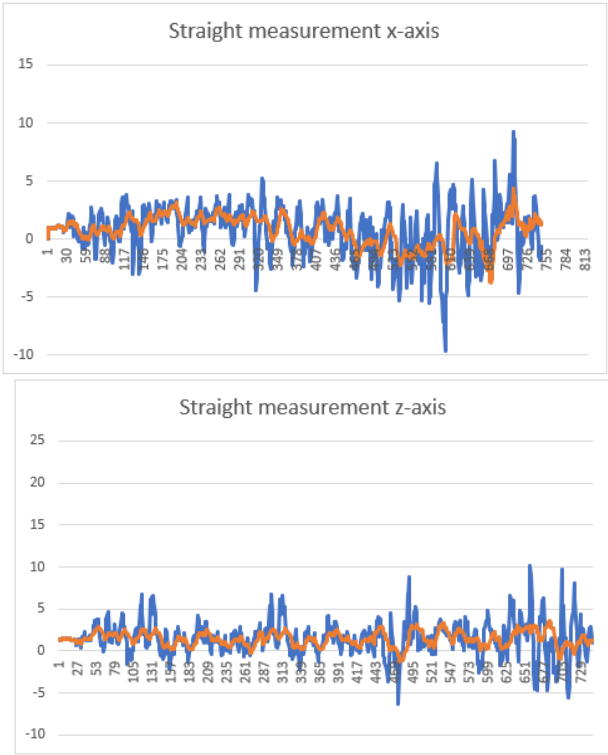
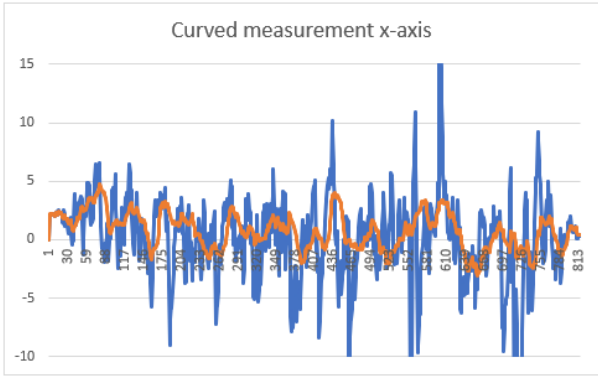


Fig. 9. Snake motion measurement on straight track



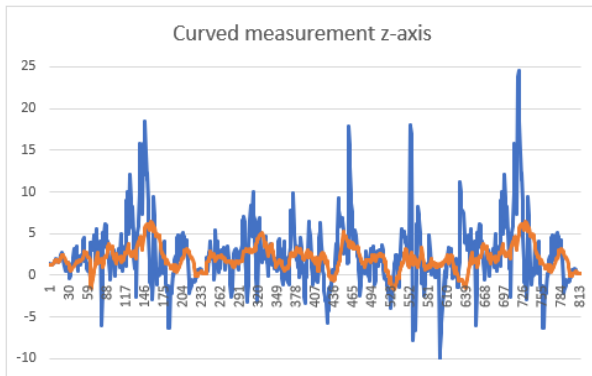


Fig. 10. Snake motion measurement on straight track

From the diagram in Figures 8 and 9, The x-axis that detects snake motion by capturing the roll movement of the flatcar. On the x-axis, the data read has the smallest value of 0.49° and the highest value of the snake movement of 2.89° . Whereas the z-axis detects the snakes motion by catching the yaw movement on the flatcar movement. From the z-axis measurement, the smallest measurements of 0.18° and the highest of 2.96° were obtained. On the x-axis, the data read has the smallest value of 0.29° and the highest value of the snake motion of 4.76° . Whereas the z-axis detects the snake movement by capturing the yaw movement on the flatcar movement. From the z-axis measurement, the smallest measurements of 0.26° and the highest of 6.44° were obtained.

5. Conclusion

The Kalman Filter Sensor Fusion algorithm is applied to the combination of the accelerometer and the gyroscope by utilising the GY251 MPU 6050 module using the Arduino Uno microcontroller performed in the IDE interface. If the variance value of the process is close to 0, then the filtering result performed by the filter is stable. The application of the filter kalman method to sensor measurements provides measurement accuracy with an average error value of 3.9% on the x axis, 3.1% on the y axis, and 5.7% on the z axis. Snake motion measurements with accelerometeor and gyroscope sensors that have been applied to the Kalman Filter Sensor Fusion algorithm yield snake motions on the flatcar occurring more when the truck passes the curvature, with the highest measurement of 2.89° on the x axis and 2.96° on the z axis when a truck runs on a straight line and the maximum measurement of 4.76° on the x axis and 6.44° on the z axis when it runs in the curve.

References

1. Sitorus, Onky Raymond. 2021. "Analisa Pemeliharaan Jalan Kereta Api Medan-Tebing Tinggi".

Fakultas Teknik – Universitas Medan Area.

2. Sakti, Mohammad Bagus Bima. 2016. "Pembuatan Alat Peraga Snake Motion." 15(2): 1–23.
3. Wawolumaja, Rudy. 2013. "Elektronika Industri & Otomasi." *Teknik Industri - Fakultas Teknik Universitas Kristen Maranatha Bandung*.
4. Iqbal, Muhammad et al. 2010. "Analisis Filter Kalman Untuk Menghapus Noise Pada Sinyal Suara." *Analisis Filter Kalman untuk Menghapus Noise pada Sinyal Suara*.
5. Nefli Yusuf, Hariadi, Arief Septian Agung Tawar. 2010. "Perbandingan Eksperimen Defleksi Batang Kantilever Berprofil Strip Terhadap Persamaan Teoritis Untuk Bahan Fe Dan Al."
6. Lai, Xiaozheng, Ting Yang, Zetao Wang, and Peng Chen. 2019. "IoT Implementation of Kalman Filter to Improve Accuracy of Air Quality Monitoring and Prediction." *Applied Sciences (Switzerland)* 9(9).
7. Ma'arif, Alfian, Iswanto Iswanto, Aninditya Anggari Nuryono, and Rio Ikhsan Alfian. 2019. "Kalman Filter for Noise Reducer on Sensor Readings." *Signal and Image Processing Letters* 1(2): 11–22.
8. K. Knothe & F. Böhm. 1999. "Investigation of contact stresses on the wheel/rail-system at steady state curving". *Vehicle System Dynamics* 33 (sup1), 616-628
9. Gaghana, Rosa Eunike Ruth, Maclaurin Hutagalung, and Herry Imanta Sitepu. 2019. "Aplikasi Sensor Fusion Untuk Mendeteksi Posisi Dan Arah Pergerakan Ponsel Pintar Di Dalam Ruangan." *Jurnal Telematika* 14(1): 19–26.
10. Ivory, Ribhi atma, Nur Kholis, Nurhayati, and Farid Baskoro. 2021. "Review Penggunaan Sensor Suara Terhadap Respon Pembacaan Skala Pada Inkubator Bayi." *Jurnal Teknik elektro* 10: 185–94.

Open Access This chapter is licensed under the terms of the Creative Commons Attribution-NonCommercial 4.0 International License (<http://creativecommons.org/licenses/by-nc/4.0/>), which permits any noncommercial use, sharing, adaptation, distribution and reproduction in any medium or format, as long as you give appropriate credit to the original author(s) and the source, provide a link to the Creative Commons license and indicate if changes were made.

The images or other third party material in this chapter are included in the chapter's Creative Commons license, unless indicated otherwise in a credit line to the material. If material is not included in the chapter's Creative Commons license and your intended use is not permitted by statutory regulation or exceeds the permitted use, you will need to obtain permission directly from the copyright holder.

